Prediction of Nonlinear Long-Term Tensile Creep of Heterogeneous Blends: Rubber-Toughened Polypropylene–Poly(styrene-*co*-acrylonitrile)

Jan Kolařík,[1] Alessandro Pegoretti,[2] Luca Fambri,[2] Amabile Penati[2]

[1]*Institute of Macromolecular Chemistry, Academy of Sciences of the Czech Republic, 162 06 Prague 6, Czech Republic*
[2]*Department of Materials Engineering, University of Trento, 38050 Trento, Italy*

ABSTRACT: The proposed predictive format for the tensile compliance, $D_b(t)$, of polymer blends is based on (1) a two-parameter equivalent box model (EBM) and (2) calculations of the phase continuity of components in blends by using modified equations of the percolation theory. The input data encompass (1) selected parameters characterizing the creep of parent polymers and (2) critical volume fractions v_{1cr} and v_{2cr} of constituents in blends (delimiting the interval of phase cocontinuity). To describe the effects of time and stress on tensile compliance, a routinely used empirical equation was found suitable. Parameters characterizing the creep of parent polymers and their blends were extracted from generalized dependencies obtained through the superposition of time dependencies of tensile compliance assessed for a series of applied stresses and reconstructed with regard to the strain-induced free-volume expansion. Reconstructed dependencies can be approximated by a straight line, which simplifies the predictive format. The comparison of experimental and calculated compliance dependencies shows that the proposed format plausibly predicts the blend creep behavior over the studied interval of 0.1–10,000 min. The upswing in blend compliance after a long period of creeping is attributed to the redistribution of stresses acting on the constituents in the course of the creep under a constant load. This format is believed to have allowed the researchers in this study to anticipate (at least semiquantitatively) the creep behavior of intended blends. © 2003 Wiley Periodicals, Inc. J Appl Polym Sci 88: 641–651, 2003

Key words: polymer blends; creep; compliance; predictive models; nonlinear viscoelasticity

INTRODUCTION

As generally recognized, potential applications of polymeric materials are frequently (co)determined by their mechanical properties; therefore, it is highly desirable to have means for anticipating these properties as functions of material composition. In our previous articles dealing with heterogeneous two- or three-component polymer blends, we proposed and verified a versatile predictive scheme for modulus (E_b),[1–9] storage (E_b'), and loss (E_b'') moduli[9]; creep compliance $[D_b(t)]$[10]; yield strength (S_{yb})[1–3,5,7,8,11]; tensile strength (S_{ub})[2,4,5,8,9]; and permeability to gases (P_b).[4,5,12,13] Also, interfacial adhesion[14] and the effect of partial miscibility[9] of the components on E_b and S_{yb} were tentatively evaluated. An essential feature of the proposed predictive format is that all considered properties of a blend are interrelated because they are calculated for a certain phase structure by applying an identical set of input parameters.

As end products made of thermoplastics are frequently exposed to a long-lasting dead load (constant external force), their dimensional stability and resistance to creep become significant characteristics. Thus, knowledge of creep behavior over appropriate intervals of time, stress, and temperature is of great practical interest.[15,16] Although the creep of many polymers has been described in the literature, relatively little is known about the creep of polymer blends, as documented even by recent monographs on polymer blends.[17–20] So far the creep behavior of blends has been studied rather sporadically[21–27]; attention has been paid mainly to blends containing a dispersed (discontinuous) minority component.[21–25] However, two-component heterogeneous blends have been treated in analogous ways as individual polymers (simple materials), and thus far no models have been attempted for predicting the creep of blends employing experimental data on the creep of constituents. Recently, we also modified[10] our predictive format for the time-dependent compliance, $D_b(t)$, of heterogeneous binary blends in the region of the linear stress–strain relationship. This format allows for (1) the creep of components and (2) phase structures encompassing a wide interval of the cocontinuity of phases. In this context it should be borne in mind[1,4–6,9,12,13,28–30] that

a minority component in two-component heterogeneous blends often assumes partial continuity at a critical volume fraction as low as $0.1 < v_{1cr}$ (or v_{cr}) < 0.2. Thus, in a wide composition interval, say, $0.15 < v_1$ (or v_2) < 0.85, phase structures with partially cocontinuous constituents are typical of polymer blends.

Many polymers, in particular crystalline ones, show nonlinear viscoelastic behavior, even at relatively low strains (1%), which means that the produced strain is no longer linearly proportional to the acting stress (the compliance rises with acting stress). The stress–strain nonlinearity observed in tensile creep experiments can be viewed[31] (at least partly) as a consequence of the strain-induced volume dilatation that occurs[15,31–33] in materials whose Poisson ratio is smaller than 0.5. The creep curves of rubber-toughened polypropylene obtained for a series of applied stresses were found to superpose if a correction was made for generated fractional free volume.[31] The objective of the current study was to combine the proposed approaches[10,31] to long-term tensile creep of impact-resistant polypropylene–poly(styrene-co-acrylonitrile) blends.[9,10] Specifically, we attempted to calculate the nonlinear creep of blends by considering the effect of strain-induced volume dilatation on the creep of components and by applying the predictive format based on the equivalent box model and modified equations of the percolation theory.

PREDICTIVE FORMAT FOR THE CREEP OF HETEROGENEOUS POLYMER BLENDS

Empirical function for the compliance of thermoplastics

The creep deformation, $\epsilon(t, \sigma, T)$, of polymers mainly depends on time (t), stress (σ), and temperature (T). In general, $\epsilon(t, \sigma, T)$ consists of three components[15,16]: (1) *elastic* (instantaneous) deformation, $\epsilon_e(\sigma, T)$; (2) *viscoelastic* (reversible) deformation, $\epsilon_v(t, \sigma, T)$; and (3) *plastic* (irreversible) deformation, $\epsilon_p(t, \sigma, T)$:

$$\epsilon(t, \sigma, T) = \epsilon_e(\sigma, T) + \epsilon_v(t, \sigma, T) + \epsilon_p(t, \sigma, T) \quad (1)$$

In practice, conditions where $\epsilon_p(t, \sigma, T) > 0$ should be avoided because any plastic deformation can be viewed as irreversible damage to an end product. The corresponding tensile compliance, $D(t, \sigma, T) = \epsilon(t, \sigma, T)/\sigma$, reads

$$D(t, \sigma, T) = D_e(\sigma, T) + D_v(t, \sigma, T) + D_p(t, \sigma, T) \quad (2)$$

Experimental creep curves are usually presented in a graphical form. If they can be fitted by an equation, then storage of experimental data, evaluation of creep rate, and interpolation or extrapolation of creep deformation are facilitated. Several attempts have been made[15,16,34–36] to simplify the description of creep under various conditions by expressing compliance as a product of independent functions of time or stress or temperature, that is, $D(t, \sigma, T) = C_p f(t)g(\sigma)h(T)$. The parameters of such empirical equations are determined *a posteriori* by fitting experimental data. Although $h(T)$ is usually identified with the Williams–Landel–Ferry (WLF) or Arrhenius equation, of numerous empirical functions proposed for $f(t)$ and $g(\sigma)$ we found[31] the following equation[37] to be suitable for both short- and long-term tensile creep of studied polymers:

$$D(t, \sigma) = W(\sigma) \, (t/\tau_{rm})^n \quad (3)$$

where $W(\sigma)$ is a function of the stress, τ_{rm} is the mean retardation time, and $0 \le n \le 1$ is the creep curve shape parameter reflecting the distribution of retardation times. Formally, similar equations were attempted in a number of articles[34,35,38–42] for the viscoelastic component of compliance, $D_v(t, \sigma) = D(t, \sigma) - D_e(\sigma)$.

Tensile creep of viscoelastic solids as a non-iso-free-volume process

The phenomenological theory of viscoelasticity has shown[15,32,43–47] that the effects of temperature and pressure on the viscoelastic behavior of polymers can be interpreted in terms of dimensionless fractional free volume, defined as

$$f = (V - V_h)/V_h \quad (4)$$

where V is the specific volume, V_h is the specific volume occupied by molecules (extrapolated from the melt to 0 K without change of phase).[47] The glassy state of polymers is viewed[15,32,43–47] as an iso-free-volume state with a constant fractional free volume, $f_g = 0.025$. Expansion of the fractional free volume at $T > T_g$ is routinely described by the following equation:

$$f = f_g + \alpha_{fv}(T - T_g) = f_g + \Delta f_T \quad (5)$$

where α_{fv} is the expansion coefficient of the free volume, which can be approximated as the difference between the coefficients above and below T_g, that is, $\alpha_{fv} = \alpha_1 - \alpha_g$.

The mechanics of solids[15,32,33] show that a body deformed in tension increases its volume if its Poisson ratio (ν) is <0.5. As long as tensile creep experiments with thermoplastics are performed at mechanically reversible strains smaller than the yield strain, the increment $\Delta V/V = (1 - 2\nu)\epsilon$ can be identified[31,33] with a contribution, Δf_ϵ, to the fractional free volume, f.

Consequently, eq. (5) can be extended to the following form:

$$f = f_g + \alpha_{fv}(T - T_g) + (1 - 2\nu)\epsilon = f_g + \Delta f_T + \Delta f_\epsilon \quad (6)$$

For the free-volume approach,[44] the available f controls the retardation (or relaxation) times:

$$\ln \tau_r = \ln \Omega + (B/f) \quad (7)$$

where Ω corresponds to the frequency of thermal motion inside a potential well and $B \approx 1$ is a numerical factor related to the ratio between the volume of a jumping segment and the volume of critical vacancy necessary for a segment jump. The effects of temperature[15,43–47] and/or compression[33] on retardation time, τ_r, can be encompassed through a shift along the time scale:

$$\log a = \log[\tau_r(f_2)/\tau_r(f_1)] \quad (8)$$

where $f_2 > f_1$ are the fractional free volumes. If the free volume is solely affected by temperature in the interval $T_g < T < (T_g + 100\ \text{K})$, then the time–temperature shift factor, $\log a_T$, mostly obeys the WLF equation,[15,43–47] the constants of which are related to the available fractional free volume $(f_g + \Delta f_T)$. From combining eq. (7) for the mean retardation time, τ_{rm}, with eqs. (6) and (8), the following equation can be obtained[31] for the time–strain shift factor, $\log a_\epsilon(t)$, defined as the ratio of the retardation times, $\tau_{rm}[\epsilon(t), T_c]$, at a strain of $\epsilon(t)$ for time (t) and $\tau_{rmi}(\epsilon_i = 0, T_c)$ for initial time, $t_i = 0$ (at a temperature T_c):

$$\log a_\epsilon(t) = -(B/2.303)[(1 - 2\nu)M\epsilon(t)/(f_g + \Delta f_{Tc})]/$$
$$\div [(1 - 2\nu)M\epsilon(t) + (f_g + \Delta f_{Tc})] \quad (9)$$

where M will be later defined as the ratio of average microscopic strain of the creeping phase or component and the measured (macroscopic) strain of a creeping specimen.

If the mean retardation time, τ_{rm}, of eq. (3) obeys eq. (8), then

$$\log D(t, \sigma) = [\log W(\sigma) - n \log \tau_{rmi} - n \log a_\epsilon(t)]$$
$$+ n \log(t) = \log C(t, \sigma) + n \log t \quad (10)$$

which can be modified to the following form:

$$\log D(t^*, \sigma) = [\log W(\sigma) - n \log \tau_{rmi}]$$
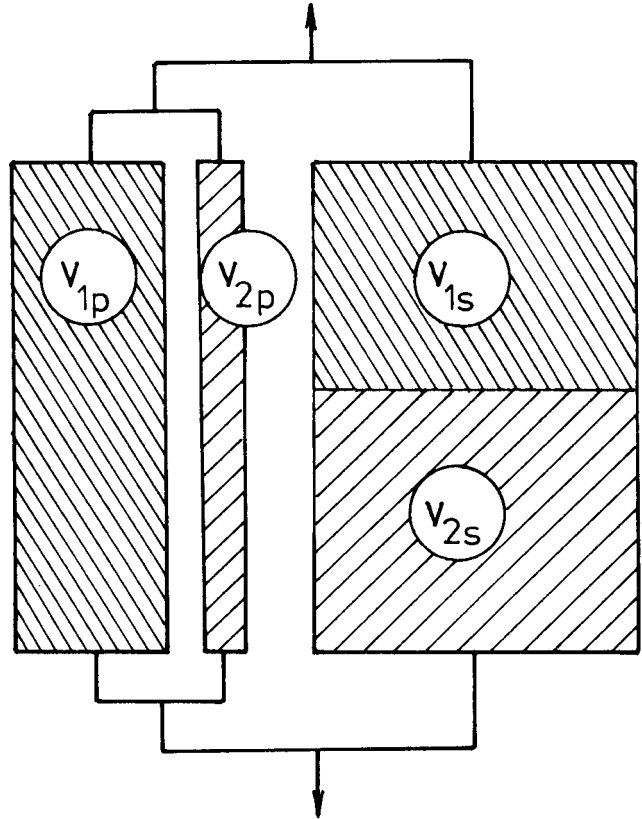$$+ n[\log t - \log a_\epsilon(t)] = \log C^*(\sigma) + n^*\log t^* \quad (11)$$

Figure 1   Equivalent box model for a binary blend 60:40

where

$$\log t^* = \log t + (B/2.303)[(1 - 2\nu)M\epsilon(t)(f_g + \Delta f_{Tc})]$$
$$\div [(1 - 2\nu)M\epsilon(t) + (f_g + \Delta f_{Tc})] \quad (12)$$

can be viewed as the "internal" time of the creep experiment. It should be noted that the value of the time–strain shift factor, $\log a_\epsilon(t)$, is not a constant for a creep curve (as in the time–temperature superposition), but rises with the creep time, a result of continuously increasing free volume in the creeping specimen. Because of this, the "internal" time, t^*, formally "accelerates" in the course of a tensile creep. The plots $\log D(t)$ versus $\log t$ and $\log D(t^*)$ versus $\log t^*$ would coincide for $\Delta f_\epsilon \rightarrow 0$, that is, for extremely low stresses and strains; thus, C^* and n^* represent the limits of C and n for the creep in a (hypothetical) pseudo-iso-free-volume state.

Compliance of heterogeneous binary blends in terms of the equivalent box model

Our predictive scheme[1–14] was based on the combination of a two-parameter equivalent box model (EBM; Fig. 1) and the data on the phase continuity of components obtained from modified equations of the percolation theory.[38,40] Ideal polymer blends are isotropic

materials with three-dimensional continuity of one or more components, so series or parallel models as well as models for orthotropic or quasi-isotropic materials are not applicable. Thus, modeling either constituent requires a more complex EBM, consisting of fractions continuous (v_{1p} or v_{2p}) and discontinuous (v_{1s} or v_{2s}) in the direction of the acting force. The constituents of the EBM are presumed to have mechanical properties of starting polymers (the model is likely to fail if the blending process produces a noticeable change in the structure and considered properties of a constituent). Compliance of the parallel [$D_p(t)$] or series [$D_s(t)$] branches of the EBM (Fig. 1) is as follows[10]:

$$(v_{1p} + v_{2p})/D_p(t) = v_{1p}/D_1(t) + v_{2p}/D_2(t) \quad (13)$$

$$1/D_s(t) = (v_{1s} + v_{2s})/[D_1(t)v_{1s} + D_2(t)v_{2s}] \quad (14)$$

The resulting compliance of heterogeneous two-component blends is given as the sum of the contributions of the parallel and series branches:

$$D_b(t) = \{v_{1p}/D_1(t) + v_{2p}/D_2(t)$$
$$+ (v_{1s} + v_{2s})^2/[D_1(t)v_{1s} + D_2(t)v_{2s}]\}^{-1} \quad (15)$$

To describe the compliance of binary blends that have one continuous and one discontinuous component (which occur in the marginal composition ranges), we modified[10] the Kerner–Nielsen equation[15] for stiffness of particulate systems. An alternative, as a first approximation, $v_{1p} = 0$, $v_{1s} = v_1$ or $v_{2p} =$ and 0, $v_{2s} = v_2$ in the EBM can be considered.

Calculation of volume fractions of the EBM

The EBM is not a self-consistent model, so it is necessary to evaluate volume fractions v_{1p}, v_{2p}, v_{1s}, and v_{2s} in an independent way in order to obtain a predictive format. Using a universal formula for the elastic modulus (or compliance) from percolation theory[30,48,49] for binary systems, we derived[1,5,12] the following equations for the volume fractions of the EBM (Fig. 1):

$$v_{1p} = [(v_1 - v_{1cr})/(1 - v_{1cr})]^q \quad (16a)$$

$$v_{2p} = [(v_2 - v_{2cr})/(1 - v_{2cr})]^q \quad (16b)$$

where v_{1cr} and v_{2cr} are the critical volume fractions (the percolation thresholds) and q is the critical universal exponent. As the EBM, shown in Figure 1, is a two-parameter model, only two of the four volume fractions are independent. The fractions v_{1s} and v_{2s} can be calculated by using the following relations:

$$v_{1s} = v_1 - v_{1p} \quad (17a)$$

$$v_{2s} = v_2 - v_{2p} \quad (17b)$$

For a three-dimensional cubic lattice, a v_{cr} of 0.156 and a q of 2 were calculated.[30,48–50] Experimental values of v_{cr} have been found[1,5,6,9,12,13,30] to occur in the interval $0.03 < v_{cr} < 0.45$, as the values of v_{cr} are profoundly affected by the relative viscosities of blend constituents. Most values of q that have been reported were in the interval 1.6–2.0, so $q = 1.8$ may be used as an average value. In general, calculations of the dependence of physical properties on blend composition that have been predicted by using the "universal" values $v_{1cr} = v_{2cr} = 0.156$ and $q = 1.8$ should be viewed as a first approximation that may not be in good accord with experimental data if v_{1cr} and/or v_{2cr} substantially deviate from their presumed value. The opposite—using a fitting procedure on experimental results to determine more precise values of v_{1cr}, v_{2cr}, and q for specific types of blends —may also be possible as soon as some experimental data on physical properties are available. In this way the EBM would become a source of quantitative information on phase duality in polymer blends.

Strain magnification factor in heterogeneous blends

The creep of a polymer that is component 1 in the blend can be reduced by blending it with a component 2 that has distinctly lower compliance (in the temperature range of the envisaged applications); however, to achieve this effect, both components in the heterogeneous blend have to be partly continuous. To take into account differing strains of the constituents of the EBM, the addition can be made of a strain-magnifying factor, M, the ratio of the microscopic strain of a constituent and the macroscopic (measured) strain of the blend. The strain of fractions v_{1p} and v_{2p} coupled in parallel (Fig. 1) would be identical with macroscopic strain, that is, $M_{1p} = M_{2p} = 1$. On the other hand, if a creep-resistant component 2 has compliance by 2–3 orders less than a component 1, it is evident that its fraction, v_{2s} (Fig. 1), coupled in series would not be perceptibly deformed in the course of blend creep ($M_{2s} \cong 0$). Therefore, the displacement in fraction v_{1s} would be practically equal to macroscopic displacement, which means the resulting strain of component 1 coupled in series would be higher than macroscopic strain ($M_{1s} > 1$); consequently, the generation of the strain-induced free volume in v_{1s} would be higher than in v_{1p}. To quantify the latter effect in the series branch, consideration must be given to the displacement values, ΔL_{1s} and ΔL_{2s} (which are additive, whereas the corresponding strains are not), and the initial lengths, L_{1s} and L_{2s}, of fractions v_{1s} and v_{2s}, respectively. Then the ratio of the microscopic and the macroscopic strains is

$$M_{1s} = (\Delta L_{1s}/L_{1s})[(\Delta L_{1s} + \Delta L_{2s})/(L_{1s} + L_{2s})] \quad (18)$$

If $\Delta L_{2s} = 0$, the following is obtained:

$$M_{1s} = (L_{1s} + L_{2s})/L_{1s} = 1 + (v_{2s}/v_{1s}) \quad (19)$$

because $L_{2s}/L_{1s} = v_{2s}/v_{1s}$ in the series branch of the EBM (Fig. 1). Creep-resistant component 2 (glassy polymer or crystalline phase) would be expected to respond to stress as a quasi-elastic material, which means mainly affecting the elastic behavior of blends. However, a creep-resistant component may have a low stress–strain linearity limit, beyond which the strain will rise more than the stress (a qualitative explanation for the experimental observation that crystalline polymers usually have a very low stress–strain linearity limit). Thus, the strain-induced free volume may affect the elastic properties of component 2 in blends rather than the time-dependent phenomena. The creep of a blend will primarily reflect the creep of (cocontinuous) component 1. To include the effect of strain-induced dilatation, this component can be characterized by the *mean* value of M_1, defined as

$$M_1 = M_{1p}(v_{1p}/v_1) + M_{1s}(v_{1s}/v_1) \quad (20)$$

Combining eqs. (19) and (20) produces

$$M_1 = (1)(v_{1p}/v_1) + [1 + (v_{2s}/v_{1s})](v_{1s}/v_1)$$
$$= (v_{1p} + v_{1s} + v_{2s})/v_1 = 1 + v_{2s}/v_1 > 1 \quad (21)$$

It is easy to show that $M_b = M_1 v_1 + M_2 v_2 = 1$, which means that the amount of strain-induced free volume corresponds to the macroscopic deformation and that the proposed concept only accounts for uneven distribution of the free volume.

A more complicated situation must be solved for RTPP–SAN blends because they consist of three phases: an amorphous phase (including the noncrystalline phase of PP and EPR rubber, which are not distinguished to simplify the model), a crystalline phase of PP, and a glassy phase of SAN. The EBM for such blends is visualized in Figure 2, in which the respective constituting phases are listed in subscript as 1*a*, 1*k*, and 2. The fractions of RTPP, listed in subscript, combine *p* and *s* in various ways according to the hierarchy of the couplings in parallel and/or in series. Following the outlined procedure, it is possible to derive the *mean* value of M_{1a} for the amorphous phase as the creeping viscoelastic constituent

$$M_{1a} = \{v_{1p} - v_{1kpp} + [1 + (v_{2s}/v_{1s})](v_{1s} - v_{1kps})\}/v_{1a}$$
$$(22)$$

where v_{1a} stands for the volume fraction of the amorphous phase in RTPP. The analogous factors M_{1k} and
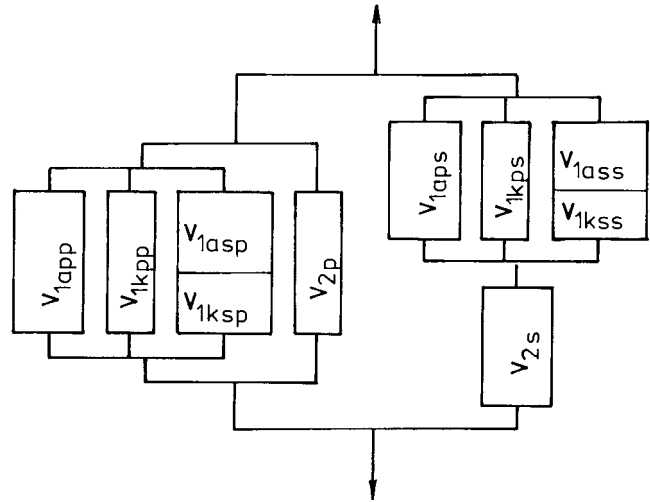

Figure 2 Equivalent box model for a binary blend consisting of a crystalline polymer 1 and an amorphous polymer 2.

M_2 can be calculated in a similar way. However, the crystalline and glassy phases are assumed to display elastic behavior without any significant time effects. We can only speculate that strain-induced Δf_e; and related factors M_{1k} and M_2 may slightly affect the corresponding compliance values, D_{1ke} and D_{2e}.

EXPERIMENTAL

Materials

Moplen EPT30R (Montell, Ferrara, Italy) was the rubber-toughened polypropylene (RTPP) used. It is a heterophase copolymer (density: 0.92 g/cm^3) that is 88% polypropylene and 12% ethylene–propylene (65:35) rubber (EPR). The poly(styrene-*co*-acrylonitrile) (SAN) used was Kostil B255 (Enichem, Mantova, Italy). It is a copolymer that is 24% acrylonitrile (density: 1.07 g/cm^3).

The polymers were mixed in a Banbury mixer (chamber 4.3 l; 164 rpm) at 175°C for 3.5 min. The produced pellets were used for feeding a Negri-Bossi injection molding machine (barrel temperature: 235°C; injection pressure: 20 MPa) to produce test specimens for the measurement of mechanical properties. Specimens used for creep studies were stored for more than a year at room temperature to avoid any effect of physical aging during measurements. Microphotographs visualizing the phase structure of selected blends were published in our previous article.[9]

Tensile creep measurements

Long-term creep was measured by using a simple apparatus equipped with a mechanical stress amplifier (lever) of 10:1. Tests in the interval 0.1–10,000 min were performed at four stress levels between 4 and 16

MPa; test specimens were used for one creep measurement only. All experiments were implemented at room temperature (between 21°C and 23°C). Mechanical preconditioning consisted of applying a stress (for 1 min) that produced a strain larger than the expected final strain of the intended long-term experiment; the following recovery (before the registered creep was initiated) took about 24 h. Specimen dimensions were—initial distance between grips: 90 mm; cross section: 10 mm × 4 mm. The length of creeping specimens was measured within an accuracy of 2 μm, or about 0.002%.

RESULTS AND DISCUSSION

In our previous article[10] we distinguished three types of creep behavior of RTPP–SAN blends on the basis of short-term creeps (lasting 100 min). For RTPP (denoted with subscript 1), the log $D_1(t)$ versus log t plot observed was (1) linear ($n_1 = 0.105$) at $\sigma < 3$ MPa; (2) still approximated by a straight line but with rising stress having increased $C_1 = C_1(\sigma)$ and $n_1 = n_1(\sigma)$ in the interval to $\sigma = 8$ MPa; and (3) showing an increase in parameter n_1 with rising stress and elapsed time of creeping at $\sigma > 10$ MPa—that is, $n_1 = n_1(\sigma, t)$. On the other hand, none of the corresponding log $D_{1v}(t)$ versus log t dependencies was found to be linear. Glassy SAN (denoted with subscript 2) showed creep behavior in contrast with that of RTPP. $D_2(t)$ was low and practically independent of stress (up to 27 MPa) and time ($C_2 = 0.29$ GPa^{-1}; $n_2 \leq 0.05$). As SAN displayed a time-independent elastic behavior, it was obvious that the viscoelastic behavior of blends was associated with the RTPP component. To apply the predictive format to the RTPP–SAN blends, it was necessary to perform the creep experiments at very low stresses in order to produce approximately linear dependencies log $D_b(t)$ versus log t, which facilitated the calculations. Such an approach is rather impractical because (1) the linearity limit is low and uncertain, (2) the relative accuracy of measurements is low, and (3) the effect of stress remains unspecified. Therefore, this article takes up the predictive format taking into account the effect of strain-induced dilatation on the creep of RTPP–SAN blends at high stresses, that is, in the region of nonlinear viscoelasticity. Parameters C_1^*, C_2^*, and n_1^*, n_2^*, obtained by fitting experimental data for parent polymers belong, to the input data in the procedure predicting the nonlinear creep of blends. As the evaluation of M factors may be difficult for some types of blends (e.g., ternary blends, binary blends of crystalline polymers), a comparison of "versatile" $M = 1$ with the M_{1a} calculated from eq. (22) was done (Table I) to determine their accuracy in fitting the experimental creep curves.

We investigated the effect of four selected stress levels (Table I) on the time dependencies of the $D(t)$

and $D_v(t)$ of RTPP and of three RTPP–SAN blends— 90:10, 80:20, and 70:30 (by weight). To reduce the number of figures, experimental results are reported only for RTPP and the 70:30 RTPP–SAN blend. The effect of stress on produced tensile strain is visualized in Figure 3, and the corresponding log $D(t)$ versus log t and log $D_v(t)$ versus log t are given in Figure 4. What is shown in Figure 4 reveals essential features of the creep behavior of the studied materials: (1) the 70:30 blend shows lower compliance because SAN forms a cocontinuous phase[9]; (2) the compliances $D(t)$ and $D_v(t)$ rise with applied stress, which may be regarded as evidence of *nonlinear* viscoelastic behavior in the interval of the applied stresses of both RTPP and the 70:30 RTPP–SAN blend; (3) dependencies log $D(t)$ versus log t are approximately linear only at the lowest stresses used,[10] whereas deviations are rising with time at higher applied stresses; (4) none of the log $D_v(t)$ versus log t dependencies can be approximated by a straight line [thus an empirical equation, log $D_v(t) = c_0 + c_1(\log t) + c_2(\log t)^2$, was used to fit the experimental data].

As soon as the strain-induced free volume was taken into account (Fig. 5), (1) the log $D_b(t^*)$ versus log t^* was fitted much better by eq. (11) than the analogous data in Figure 4 was by eq. (10) and (2) the dependencies log $D_b(t^*)$ versus log t^* or log $D_{bv}(t^*)$ versus log t^* found for different stresses were approximately superposed (Fig. 5), indicating a *quasi-linear stress–strain* relationship in the coordinates including "internal" time, t^* [stress-strain linearity has nothing to do with the linearity of the log $D_b(t^*)$ versus log t^* plot]. Summarized in Table I are the effects of parameter M_{1a}, calculated from eq. (22), on the extracted parameters C^* and n^* and on the accuracy of the fitting of the experimental data using eq. (11). ($M = 0$ or $M = 1$ means the strain-induced free volume was ignored or viewed as evenly distributed throughout the test specimen.) As can be seen, log C^* slightly decreased at $M = 1$, but the estimated standard deviation (esd) was not systematically and substantially affected. It can be seen from comparing the n for $M = 0$ with the n^* for $M = 1$ that n^* was lower by about 20%, but the corresponding esd was much lower, which means the fitting of the experimental data was markedly improved (cf. Figs. 4 and 5). This tendency is also confirmed by increased reliability values, R^2. Introduction of M_{1a} calculated from eq. (22) led—in comparison with $M = 1$—to a slight decrease in n^* and esd and a small increase in R^2. Thus, it can be concluded that the substitution of $M = 0$ by $M = 1$ substantially improved the accuracy of the fitting of the experimental data. The replacement of $M = 1$ by M_{1a} improved the accuracy even more in the fitting procedure, but the differences were much less than in the previous case. Thus, the creep dependency obtained by the time-strain superposition of a set of creep curves at $M = 1$

TABLE I
Effect of Strain-Induced Free-Volume Expansion on Parameters of Eqs. (10) and (11)

Stress	log C	n	R^2	log C*	n*	R^2	log C*	n*	R^2
				Rubber-toughened polypropylene					
MPa	M = 0			M = 1			M = 1.47		
3.99	−0.098	0.092	0.9960	−0.118	0.086	0.9972	−0.127	0.084	0.9975
6.72	−0.050	0.106	0.9792	−0.114	0.092	0.9881	−0.104	0.087	0.9906
8.54	−0.017	0.154	0.9891	−0.072	0.110	0.9981	−0.092	0.101	0.9987
12.09	−0.004	0.189	0.9843	−0.086	0.114	0.9983	−0.114	0.103	0.9988
Mean	−0.097	0.135	0.9872	−0.098	0.101	0.9954	−0.109	0.094	0.9964
e.s.d.	0.021	0.044		0.022	0.014		0.015	0.009	
r (%)	21.6	32.6		22.4	13.9		13.8	9.7	
				Blend RTPP/SAN = 90/10					
MPa	M = 0			M = 1			M = 1.55		
4.86	−0.198	0.085	0.9917	−0.216	0.080	0.9938	−0.225	0.078	0.9946
8.03	−0.091	0.082	0.9880	−0.126	0.073	0.9923	−0.141	0.070	0.9935
9.71	−0.054	0.120	0.9793	−0.112	0.096	0.9915	−0.134	0.088	0.9938
12.23	−0.026	0.140	0.9830	−0.103	0.099	0.9970	−0.132	0.090	0.9981
Mean	−0.092	0.106	0.9855	−0.114	0.087	0.9937	−0.158	0.082	0.9950
e.s.d.	0.075	0.028		0.052	0.012		0.046	0.010	
r (%)	81.5	26.4		45.6	13.8		28.8	12.2	
				Blend RTPP/SAN = 80/20					
MPa	M = 0			M = 1			M = 1.69		
6.69	−0.158	0.054	0.9873	−0.175	0.051	0.9893	−0.186	0.050	0.9903
9.44	−0.136	0.061	0.9921	−0.164	0.056	0.9941	−0.180	0.054	0.9949
12.14	−0.120	0.084	0.9792	−0.168	0.072	0.9879	−0.192	0.067	0.9904
16.11	−0.127	0.124	0.9237	−0.205	0.092	0.9756	−0.240	0.083	0.9821
Mean	−0.135	0.081	0.9855	−0.178	0.068	0.9867	−0.200	0.063	0.9894
e.s.d.	0.016	0.032		0.018	0.018		0.027	0.015	
r (%)	11.8	39.5		10.1	26.5		13.4	23.8	
				RTPP/SAN = 70/30					
MPa	M = 0			M = 1			M = 1.74		
8.03	−0.187	0.040	0.9967	−0.203	0.039	0.9974	−0.211	0.037	0.9973
12.02	−0.234	0.056	0.9830	−0.261	0.052	0.9868	−0.277	0.050	0.9874
13.92	−0.226	0.065	0.9727	−0.261	0.059	0.9802	−0.281	0.056	0.9832
16.07	−0.207	0.097	0.9387	−0.263	0.079	0.9690	−0.292	0.072	0.9764
Mean	−0.214	0.064	0.9855	−0.247	0.057	0.9833	−0.265	0.054	0.9861
e.s.d.	0.021	0.023		0.029	0.017		0.037	0.014	
r (%)	9.8	36.0		11.7	29.8		14.0	26.4	

C, n: parameters of eq. (10) for real time t, cf. Fig. 4.
C^*, n^*: parameters of eq. (11) for "internal" time t^* for $M > 1$ (cf. Fig. 5).
R, R^*: reliability values.
e.s.d.: estimated standard deviation of individual measurements
$r = [(\text{mean})/(\text{e.s.d.})]\,100.$

can be regarded as the simplest yet still plausible coverage of the effect of strain-induced free volume and as suitable for complex phase structures.

It can be seen in Figure 5(a) that superposing dependencies $\log D(t^*)$ versus $\log t^*$ for RTPP follows a straight line, so they can be well fitted by eq. (3). This experimental fact is favorable to the prediction of the creep behavior of blends because $D_b(t)$ is a much more

practical function than $D_{bv}(t)$. On the other hand, from Figure 5(b) a noticeable upswing of $\log D_b(t^*)$ with $\log t^*$ is evident for the 70:30 blend, which becomes more pronounced at higher stresses, even at $M_{1a} = 1.74$. This behavior is in contrast with that of the parent polymers, as RTPP shows a linear $\log D(t^*)$ versus $\log t^*$ dependence, whereas time effects in the creep of SAN are negligible.[10] The reason for the "nonaddi-
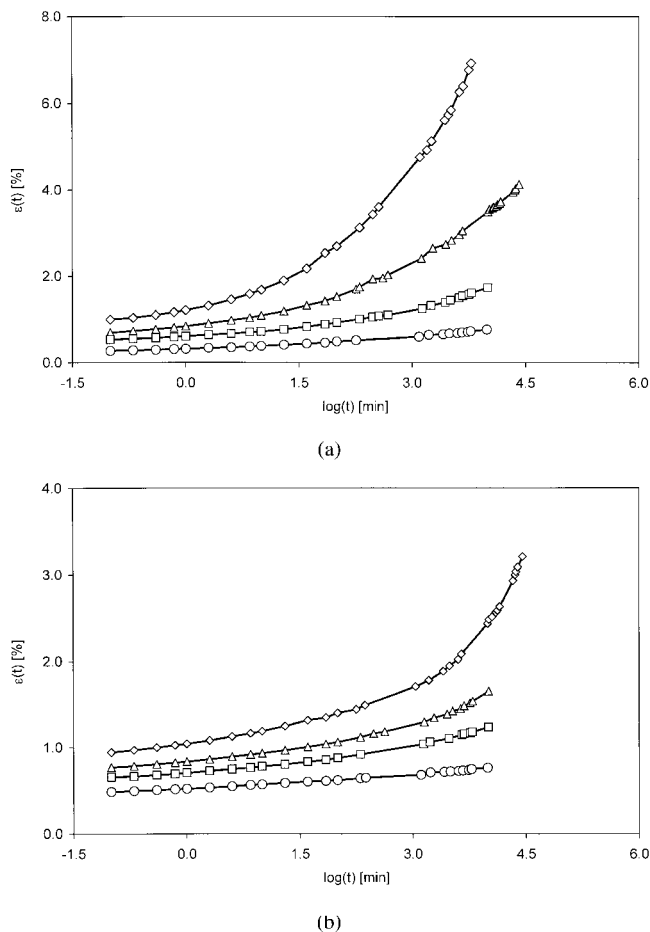
Figure 3 Effect of stress on tensile strain of (a) rubber-toughened polypropylene (RTPP) and (b) blend RTPP–SAN = 70:30. Applied tensile stress (MPa): (a) ○: 4; □: 6.7; △: 8.5; ◇: 12.1; (b) ○: 8; □: 12; △: 13.9; ◇: 16.1.

tive" behavior of the blend is the much higher stress acting on the series fraction v_{2p} of SAN (Fig. 1) than that acting on v_{1p}, which increases with the creep time as the compliance of RTPP rises. This trend can be semiquantitatively evaluated with the EBM (Fig. 1). This evaluation shows that the action of effective stress (σ_b) in a blend consists of three contributions coupled in parallel (to simplify the problem, we assumed that in the series branch only the RTPP block, v_{1s}, was deformed):

$$\sigma_b = \epsilon/D_b = \epsilon[v_{1p}/D_1 + v_{2p}/D_2 + (v_{1s} + v_{2s})/D_1]$$

$$= \epsilon[(v_{1p} + v_s)/D_1 + v_{2p}/D_2] \quad (23)$$

where $v_s = v_{1s} + v_{2s}$. The stress–strain relationships derived for two-component systems coupled in parallel show[16] that

$$\sigma_2/\sigma_1 = E_2/E_1 = D_1/D_2 \quad (24)$$

where σ_1 and σ_2 are the stresses acting on components 1 and 2, respectively, and E_1 and E_2 are the respective moduli of the components. Combining eqs. (23) and (24) produces

$$\sigma_2 = \sigma_b/[v_{2p} + (v_{1p} + v_s)(D_2/D_1)] \quad (25a)$$

$$\sigma_1 = \sigma_b/[v_{1p} + v_s + v_{2p}(D_2/D_1)] \quad (25b)$$

The studied blends were found to be characterized[9] by $v_{1cr} = 0.16$, $v_{2cr} = 0.13$, and $q = 1.2$. If these values are introduced into eqs. (16) and (17), the following volume fractions are obtained for the 70:30 blend ($v_2 = 0.26$): $v_{1p} = 0.63$; $v_{2p} = 0.11$; $v_{1s} = 0.10$; $v_{2s} = 0.16$. After 1 min or creeping or 10,000 min of creeping (Fig. 4), the typical value of the compliance D_1 was about 1 or 3 GPa^{-1}; $D_2 = 0.3$ GPa^{-1} can be considered as virtually independent of time.[10] From introducing these values into eqs. (25) it can be seen that $\sigma_2 = 2.65\ \sigma_b$ and $\sigma_1 = 0.796\ \sigma_b$ or $\sigma_2 = 5.02\ \sigma_b$ and $\sigma_1 = 0.503\ \sigma_b$ after 1 min or creeping or 10,000 min of creeping. These
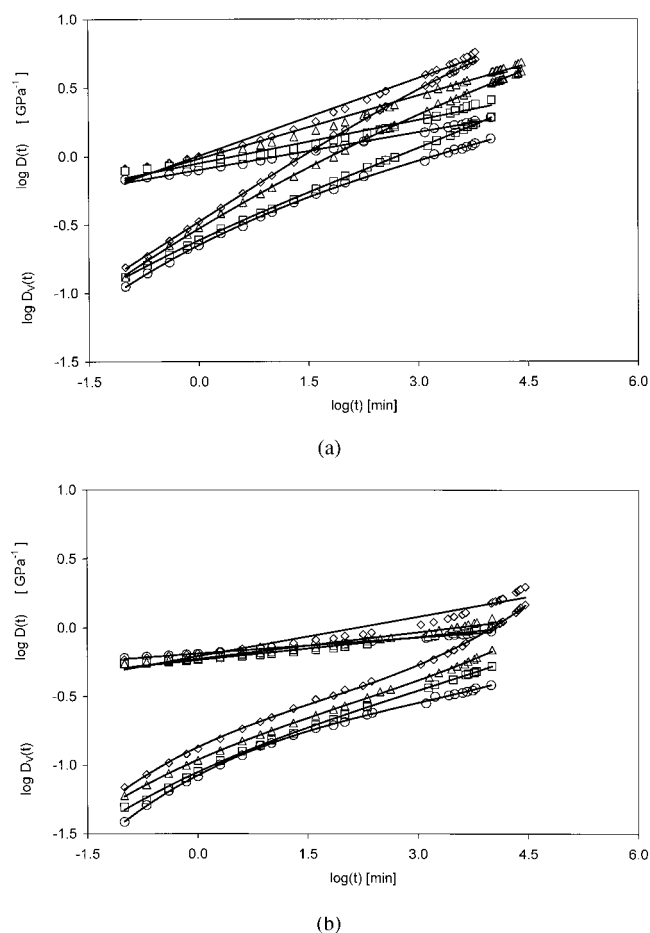

Figure 4 Compliance [$D(t)$; upper curves] and viscoelastic component of compliance [$D_v(t)$; lower curves] of (a) rubber-toughened polypropylene (RTPP) and (b) 70:30 RTPP–SAN blend for stress magnification factor $M = 0$ (for meaning of the symbols, see Fig. 3).
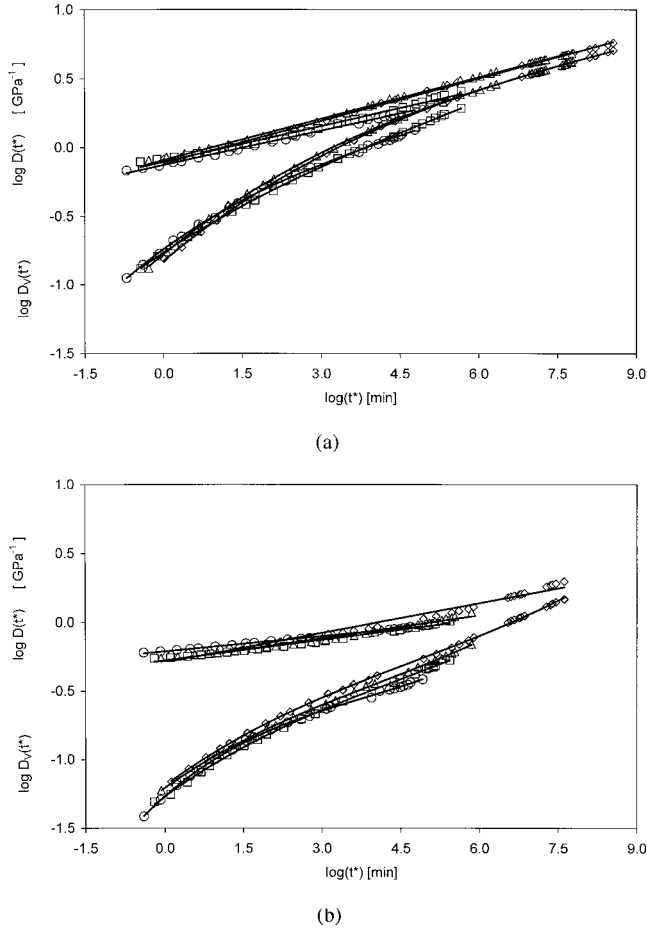
Figure 5 Compliance [$D(t)$; upper curves] and viscoelastic component of compliance [$D_v(t)$; lower curves] of (a) rubber-toughened polypropylene (RTPP) and (b) 70:30 RTPP–SAN blend for stress magnification factor $M = 1.47$ and 1.74, respectively (for meaning of the symbols, see Fig. 3).

informative values show that in our study the average stress acting on the RTPP component in blends was perceptibly lower than the effective stress, σ_b. In contrast, if the highest stress applied in the creep experiment with the 70:30 blend were $\sigma_b = 16$ MPa (Figs. 3–5, Table I), the stress acting on the SAN phase coupled in parallel would increase with time and attain an σ_2 value of about 80 MPa and a strain (ϵ_2) of 3.3% at the end of a long-term creep experiment. The latter values exceed the tensile strength, $\sigma_{2u} = 70.8$ MPa, and the strain at break, $\epsilon_{2u} = 2.8\%$, found in previous

stress–strain experiments (performed at a strain rate of 8.3%) for macroscopic specimens of SAN.[9] Thus, it can be inferred that the cause of the blend compliance upswing with time was not a particular time dependence value of $n_b{}^*$ but rather was an increase in log $C_2{}^*(\sigma)$ because of the steadily rising stress acting on the SAN fraction in blends coupled in parallel. In other words, the dependence log $D_2(t^*, \sigma_2) = $ log $C_2{}^*(\sigma_2) + n_2{}^*$ log t^* went above the straight line envisaged by eq. (11) because stress, σ_2, rose during the creep despite the σ_b remaining constant. The opposite trend in the RTPP (majority) component was much less dramatic. Redistribution of stresses acting on co-continuous components is probably an inherent feature of blends, which may make the analysis and/or prediction of the blend creep behavior much more difficult than it is for simple materials.

On the basis of the acquired knowledge, the prediction of compliance curves of blends can be predicted, using experimental data for parent polymers, that is, log $D_1 = $ log $C_1{}^* + n_1{}^*(\log t^*)$ and log $D2 = $ log $C_2{}^* + n_2{}^*(\log t^*)$. In addition, the validity of log $D_b = $ log $C_b{}^* + n_b{}^*(\log t^*)$ is assumed for blends. Introducing these relations into eq. (15) and assuming $t = 1$, the relation between $C_1{}^*$, $C_2{}^*$, and $C_b{}^*$ can be obtained:

$$C_b^* = [(v_{1p}/C_1^*) + (v_{2p}/C_2^*) + (v_{1s} + v_{2s})^2/(v_{1s}C_1^* + v_{2s}C_2^*)]^{-1}. \quad (26)$$

The compliance of a blend (for $t \neq 1$) is then given as

$$\log D_b(t^*) = \log\{[(v_{1p}/C_1^{*}t^{*y}) + (v_{2p}/C_2^{*}t^{*z}) + (v_{1s} + v_{2s})^2 \div (v_{1s}C_1^{*}t^{*y} + v_{2s}C_2^{*}t^{*z})]^{-1}\} = \log C_b^* + n_b^* \log t^*, \quad (27)$$

where $y = n_1{}^*$ and $z = n_2{}^*$. The relation between $n_1{}^*$, $n_2{}^*$, and $n_b{}^*$ assumes the following form:

$$n_b = \{-\log C_b^* - \log[(v_{1p}/C_1^{*}t^{*y}) + (v_{2p}/C_2^{*}t^{*z}) + (v_{1s} + v_{2s})^2/(v_{1s}C_1^{*}t^{*y} + v_{2s}C_2^{*}t^{*z})]\}/\log t \quad (28)$$

Although Table I shows that the experimentally found log $C_1{}^*$ slightly depended on stress, we have made the simplifying assumption that $C_1{}^* = 0.80$ GPa^{-1} (average value in Table I found for $M = 1$); $C_2{}^* = 0.29$ GPa^{-1} was found in the previous article.[10]

TABLE II
Parameters C_b^* and n_b^* of eq. (11) Determined from Long-Term Creep Experiments or Calculated from eqs. (26) and (28) for Blends RTPP/SAN

Volume fraction of SAN	Experiment		Theory			
	C_b^* (GPa^{-1})	n_b^*	C_b^* (GPa^{-1})	n_b^* (10 min)	n_b^* (10^3 min)	n_b^* (10^5 min)
0.087	0.77	0.087	0.73	0.092	0.093	0.093
0.176	0.66	0.068	0.66	0.082	0.081	0.081
0.268	0.57	0.053	0.59	0.068	0.066	0.063

Table II shows that the values of C_b^* calculated from eq. (26) are in a good accord with the experimental values for the blends. An indication is provided in eq. (28) that the parameter n_b^*, predicted by the EBM, is a function of the creep time, though n_1^* and n_2^* are assumed to be time-independent constants; however, the decrease in calculated n_b^* with the creep time was negligible. For the 90:10 RTPP–SAN blend, where $v_2 = 0.087 < v_{2cr} = 0.13$, a simplifying assumption was used: $v_{2p} = 0$, $v_{2s} = v_2$. As can be seen (Table II), the calculated n_b^* is somewhat higher than the experimental ones, but their dependencies on composition are quite parallel.

The essential feature of the proposed format is that it makes possible the prediction of the dependency log $D_b(t)$ versus log t for a selected stress (in the interval up to the yield stress) and blend composition. The parameters log C_b^* and n_b^*, precalculated from eqs. (26) and (28), would allow using eq. (11) to calculate compliance, $D_b(t^*)$, for any selected "internal" time, t^*. To obtain a plot of log $D_b(t)$ against the corresponding "real" time, t, eq. (9) can be modified by introducing $\epsilon(t) = \sigma D(t)$:

$$\log a_\epsilon = -(B/2.303)[(1 - 2\nu)M\sigma D(t)/(f_g + \Delta f_{Tc})]$$
$$\div [(1 - 2\nu)M\sigma D(t) + (f_g + \Delta f_{Tc})] \quad (29)$$

Then, according to eq. (8),

$$\log t = \log t^* + \log a_\epsilon \quad (30)$$

In this way the data points of the log $D_b(t)$ versus log t curve can be calculated for a selected tensile stress, σ_b, employing the same input parameters—B, M, ν, T_g, f_g, Δf_{Tc}, and α_{fv}—previously used in eqs. (9), (11), and (12).

Now it can be verified to what extent the dependency log $D_b(t)$ versus log t, which was projected by using the calculated *constants* C_b^* and n_b^* (Table II), can fit experimental data. Figure 6 shows the experimental long-term compliances of the 70:30 blend for $\sigma_b = 13.9$ or 16.1 MPa (cf. Fig. 4) compared with the compliance for $\sigma_b = 15$ calculated by using log $C_b^* = -0.231$ and $n_b^* = 0.066$ (Table II). As can be seen, the calculated curve is very close to a straight line: the predicted compliance is somewhat higher than the experimental data up to log $t = 3.5$, whereas at longer periods the trend is opposite. Obviously, the model cannot predict the compliance upswing at long periods because the redistribution of the stress acting on the blend's constituents is difficult to take into account. At lower stresses, for which the compliance upswing at long times is not so conspicuous (Fig. 4), the predicted compliance would be more accurate over the whole time interval.
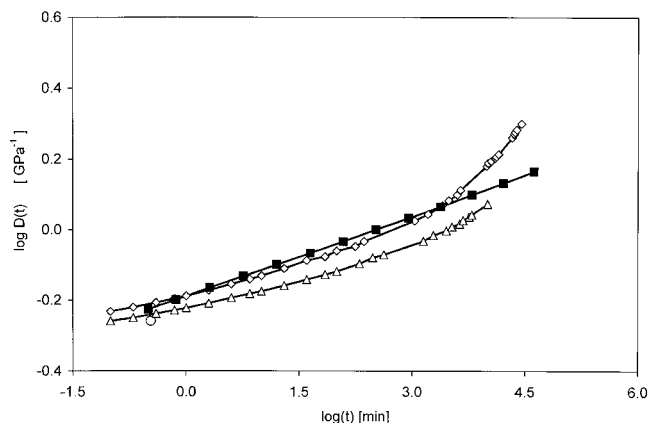

Figure 6 Compliance [$D_b(t)$] of the 70:30 RTPP–SAN blend as a function of time at tensile stress. Experimental data—△: 13.9 MPa; ◇: 16.1 MPa. Calculated data—■: 15 MPa. Input parameters: $C_1 = 0.88$ GPa^{-1}, $C_2 = 0.29$ GPa^{-1}, $n_1 = 0.105$, $n_2 = 0.005$ (Table I); $v_{1cr} = 0.16$, $v_{2cr} = 0.13$, $q_1 = q_2 = 1.2$.[9]

CONCLUSIONS

The previously proposed predictive format for time-dependent compliance, $D_b(t)$, of polymer blends has been extended in this study for long-term tensile creep in the region of the nonlinear stress–strain relationship. The format input data encompassed: (1) parameters characterizing the creep of parent polymers, which can be extracted from a generalized dependence obtained through the superposition of time dependencies of tensile compliance assessed for a series of stresses and reconstructed for strain-induced free-volume expansion; and (2) critical volume fractions v_{1cr} and v_{2cr} of constituents in blends (delimiting the interval of phase cocontinuity). By using modified equations of the percolation theory, these data were entered into the predictive format for compliance $D_b(t)$ of the polymer blends based on a two-parameter equivalent box model (EBM) and on calculations of the phase continuity of components in blends.

To describe the effects of time and stress on compliance of RTPP [$D_1(t)$], of SAN [$D_2(t)$], and of blends [$D_b(t)$], a routinely used empirical equation has been found suitable. The superposition of the reconstructed time dependencies of the compliance is quite analogous to that in the region of linear viscoelasticity. Reconstructed dependencies can be approximated by a straight line, which simplifies the predictive format. The applicability of the proposed approach was verified on RTPP–SAN blends whose components had markedly different viscoelastic properties. A comparison of experimental and calculated compliance dependencies on time showed that the proposed format predicts the blend creep behavior fairly well over the studied interval, 0.1–10,000 min. Upswing of the blend compliance after a long period of creeping (say, 5000 min), which has been attributed to the redistribution

of stresses acting on the constituents in the course of the creep under a constant load, is difficult to evaluate quantitatively because data are not accessible on the SAN creep at extremely high stresses. Thus, the combination of (1) the concept of tensile creep as a non-iso-free-volume process, (2) the EBM, and (3) the percolation approach to phase continuity in polymer blends constitute a solid predictive format suitable for the tensile creep of heterogeneous polymer blends. This format is believed to allow those conducting experiments to anticipate (at least semiquantitatively) the creep behavior of intended blends consisting of two creeping components or containing a creep-resistant component enhancing dimensional stability.

References

1. Kolařík, J. Polym Eng Sci 1996, 36, 2518.
2. Kolařík, J.; Lednický, F.; Locati, G. G.; Fambri, L. Polym Eng Sci 1997, 37, 128.
3. Kolařík, J. Polym Compos 1997, 18, 433.
4. Horák, Z.; Kolařík, J.; Šípek, M.; Hynek, V.; Večerka, F. J Appl Polym Sci 1998, 69, 2615.
5. Kolařík, J. Eur Polym J 1998, 34, 585.
6. Matějka, L.; Duch, O.; Kolařík, J. Polymer 1999, 41, 1449.
7. Kolařík, J. J Macromol Sci-Phys 2000, B39, 53.
8. Kolařík, J.; Fambri, L.; Pegoretti, A.; Penati, A. Polym Adv Technol 2000, 11, 1.
9. Kolařík, J.; Pegoretti, A.; Fambri, L.; Penati, A. J Polym Res 2000, 7, 1.
10. Kolařík, J.; Pegoretti, A.; Fambri, L.; Penati, A. Polym Eng Sci 2002, 42, 161.
11. Kolařík, J. Polym Networks Blends 1995, 5, 87.
12. Kolařík, J.; Geuskens, G. Polym Networks Blends 1997, 7, 13.
13. Kolařík, J.; Fambri, L.; Pegoretti, A.; Penati, A. Polym Eng Sci 2000, 40, 127.
14. Kolařík, J. Polymer 1996, 37, 887.
15. Nielsen, L. E.; Landel, R. F. Mechanical Properties of Polymers and Composites; M. Dekker: New York, 1994.
16. 16. Crawford, R. J. Plastics Engineering; Butterworth-Heinemann: Oxford, U.K., 1998.
17. Utracki, L. A. Polymer Alloys and Blends; Hanser Publishing: Munich, Germany, 1990.
18. Folkes, M. J.; Hope, P. S. Polymer Blends and Alloys; Chapman & Hall: Cambridge, U.K., 1993.
19. Sperling, L. H. Polymeric Multicomponent Materials; Wiley: New York, 1997.
20. Paul, D. R.; Bucknall, C. B., Eds. Polymer Blends; Wiley: New York, 1999.
21. Bucknall, C. B.; Drinkwater, L. C. J Mater Sci 1973, 8, 1800.
22. Bucknall, C. B.; Page, C. J. J Mater Sci 1982, 17, 808.
23. Gramespacher, H.; Meissner, J. J Rheol 1995, 39, 151.
24. Mariani, P.; Frassine, R.; Rink, M.; Pavan, A. Polym Eng Sci 1996, 36, 2750.
25. Lee, A.; McKenna, G. B. J Polym Sci B: Polym Phys 1997, 35, 1167.
26. Xu, B.; Simonsen, J.; Rochefort, W. E. J Appl Polym Sci 2000, 76, 1100.
27. Lu, J. P.; Burn, L. S.; Tiganis, B. E. Polym Eng Sci 2000, 40, 2407.
28. Utracki, L. A. J Rheol 1991, 35, 1615.
29. Lyngaae-Jorgensen, J.; Utracki, L. A. Makromol Chem, Macromol Symp 1991, 48/49, 189.
30. Lyngaae-Jorgensen, J.; Kuta, A.; Sondergaard, K.; Poulsen, K. V. Polym Networks Blends 1993, 3, 1.
31. Kolařík, J. J Polym Sci: Polym Phys, submitted
32. Riande, E.; Diaz-Calleja, R.; Prolongo, M. G.; Masegosa, R. M.; Salom, C. Polymer Viscoelasticity; Marcel Dekker: New York, 2000.
33. Ferry, J. D.; Stratton, R. A. Kolloid Z 1960, 171, 107.
34. Schlimmer, M. Rheol Acta 1979, 18, 62.
35. Boey, F. Y. C.; Lee, T. H.; Khor, K. A. Polym Test 1995, 14, 425.
36. Li, J. X.; Cheung, W. L. J Appl Polym Sci 1995, 56, 881.
37. Garbella, R. W.; Wachter, J.; Wendorff, J. H. Prog Colloid Polym Sci 1985, 71, 164.
38. Findley, W. N. Polym Eng Sci 1987, 27, 582.
39. Dillard, D. D.; Straight, M. R.; Brinson, H. F. Polym Eng Sci 1987, 27, 116.
40. Migliaresi, C.; Fambri, L.; Kolařík, J. Biomaterials 1994, 15, 875.
41. Liou, W. J.; Tseng, C. I. Polym Compos 1997, 18, 492.
42. Carriere, C. J.; Bank, D.; Malanga, M. J Appl Polym Sci 1998, 67, 1177.
43. Bueche, F. Physical Properties of Polymers; Interscience: New York, 1962.
44. McCrum, N. G.; Read, B. E.; Williams, G. Anelastic and Dielectric Effects in Polymeric Solids; Wiley: London, 1967.
45. Aklonis, J. J.; MacKnight, W. J.; Shen, M. Introduction to Polymer Viscoelasticity; Wiley-Interscience: New York, 1972.
46. Ward, I. M.; Hadley, D. W. An Introduction to the Mechanical Properties of Solid Polymers; Wiley: Chichester, UK, 1993.
47. Rodriguez, F. Principles of Polymer Systems; Taylor & Francis: Washington, DC, 1996.
48. De Gennes, P. G. J Phys Lett (Paris) 1976, 37, L1.
49. Hsu, W. Y.; Wu, S. Polym Eng Sci 1993, 33, 293.
50. Sax, J.; Ottino, J. M. Polym Eng Sci 1983, 23, 165.